Oral administration of glucose promotes intracellular partitioning of fatty acid toward storage in white but not in red muscle

Keld Fosgerau, Christian Fledelius[1], Kent E Pedersen[1], Jesper B Kristensen[1], Jens R Daugaard[1], Miguel A Iglesias[2], Edward W Kraegen[2] and **Stuart M Furler[2]**

In vivo Pharmacology, Rheoscience, Ledøje Bygade 23B, DK-2765 Ledøje-Smørum, Denmark

[1]Novo Nordisk Discovery and Development, Novo Nordisk A/S, Novo Nordisk Park, DK-2760 Maaloev, Denmark

[2]Garvan Institute of Medical Research, 384 Victoria Street, Sydney NSW 2010, Australia

(Requests for offprints should be addressed to K Fosgerau; Email: kf@rheoscience.com)

Abstract

Lipid accumulation in non-adipose tissues is strongly associated with the metabolic syndrome, possibly due to aberrant partitioning of intracellular fatty acids between storage and oxidation. In the present study, we administered the non-metabolizable fatty acid analog [9,10-^{3}H]-(*R*)-2-bromopalmitate, and authentic ^{14}C-palmitate to conscious rats, in order to directly examine the initial intracellular fate of fatty acids in a range of insulin-sensitive tissues, including white and red muscles, liver, white adipose tissue, and heart. Rats were studied after administration of an oral glucose load to examine the effect of physiological elevation of glucose and insulin. The tracer results showed that glucose administration partitioned fatty acid toward storage in white muscle (storage:uptake ratios, vehicle vs glucose; $0{\cdot}64 \pm 0{\cdot}02$ vs $0{\cdot}92 \pm 0{\cdot}09$, $P < 0{\cdot}05$), and in liver ($0{\cdot}66 \pm 0{\cdot}07$ vs $0{\cdot}98 \pm 0{\cdot}04$, $P < 0{\cdot}05$), but not in red muscle ($1{\cdot}18 \pm 0{\cdot}07$ vs $1{\cdot}36 \pm 0{\cdot}11$, $P =$ not significant). These results demonstrate the physiological relevance of the so-called 'reverse' Randle cycle, but surprisingly show that it may be more important in white rather than oxidative red muscle.

Journal of Endocrinology (2006) **190,** 651–658

Introduction

It is now apparent that disturbances in lipid metabolism contribute significantly to insulin resistance and other aspects of the metabolic syndrome. The tissues that primarily determine the whole-body glucose homeostasis and insulin response are skeletal muscle and liver. A large number of studies in animals and humans have now associated excess accumulation of lipid in these tissues with insulin resistance (Hegarty *et al.* 2003). Moreover, excess intracellular fatty acids and their derivatives have been shown to interfere with glucose metabolism via a number of mechanisms, including substrate competition, inhibition of insulin signaling pathways, and modulation of gene transcription processes (Hegarty *et al.* 2003). However, the processes leading to excess lipid accumulation in non-adipose tissue are not completely understood. It is possible that lipid accumulates not because of an increase in the uptake of fatty acids but because of a reduction in their utilization as fuel (Kelley & Goodpaster 2001). Consequently, there is considerable interest in defining the processes that control the intracellular partitioning of free fatty acid (FFA) between oxidation and storage pathways.

A key control point is situated where activated fatty acid (FA-CoA) enters the mitochondrial matrix. This entry is facilitated by the enzyme carnitine palmitoyl-transferase I (CPT-I), which is inhibited by malonyl-CoA. Production of malonyl-CoA is catalyzed by acetyl-CoA carboxylase (ACC) and derived from acetyl-CoA, a product of fatty acid oxidation that is generated in the mitochondria but has access to the cytosol. Apart from its role as a feedback regulator of fatty acid oxidation, this control system can also be activated by other stimuli. Thus, increased oxidative glucose metabolism also elevates acetyl-CoA levels leading to increased malonyl-CoA and subsequent inhibition of fatty acid oxidation (Sidossis *et al.* 1996). In addition, AMP-activated protein kinase (AMPK); an enzyme activated in most cells in response to a perceived energy deficit, phosphorylates and thereby inhibits ACC resulting in stimulation of fatty acid oxidation (Hardie & Carling 1997).

The seminal study of Sidossis *et al.* (1996) in humans clearly demonstrated a decrease in whole-body fatty acid oxidation after glucose flux was increased for 5 h by a hyperglycemic/hyperinsulinemic clamp, providing the basis for what has become known as the 'reverse' Randle cycle or reverse glucose/fatty acid cycle. However, it might be expected that a consequence of a decrease in fatty acid oxidation in oxidative tissues, such as muscle, would be an increase in the fraction of FFA uptake that is directed to storage. In this regard, our own recent studies in rats, using shorter protocols ($\sim$2 h), have been equivocal. Under euglycemic/hyperinsulinemic clamp conditions, there was evidence that FFA was partitioned

DOI: 10.1677/joe.1.06809
0022–0795/06/0190–651
Online version via http://www.endocrinology-journals.org

toward storage in liver but not in skeletal muscle (Hegarty *et al.* 2002). In addition, pharmacological activation of AMPK induced an expected partitioning of FFA toward oxidation in white, but not red muscle (Iglesias *et al.* 2004). Taken together, these results suggest that the degree of modulation of FFA oxidation that can be achieved via the AMPK/malonyl-CoA network may depend on the quantitative and qualitative nature of the stimulus applied.

The aim of the present study was to determine whether, and in what tissues, intracellular partitioning of FFA could be modulated by a mild physiological stimulus. In particular, we wished to study the response to physiologically elevated plasma glucose and insulin caused by an oral administration of a glucose load. This stimulus was chosen to simulate conditions during the post-prandial absorptive phase. Our experiments were performed in rats, using the bromopalmitate/palmitate double tracer technique (Oakes *et al.* 1999), which involves simultaneous administration of the partly metabolizable FFA tracer [9,10-^{3}H]-(*R*)-2-bromopalmitate (^{3}H-*R*-BrP) and the fully metabolizable FFA tracer ^{14}C-palmitate (^{14}C-P). This technique, as well as yielding measurements of tissue-specific rates of FFA clearance, uptake and storage, also directly quantifies initial intracellular partitioning of FFA *in vivo* (Oakes *et al.* 1999, Hegarty *et al.* 2002, Oakes & Furler 2002).

Materials and Methods

Animals

Six-week-old male Sprague–Dawley rats were obtained from Taconic MB (Ry, Denmark). Prior to the experiments, the rats were housed under constant humidity in a temperature-(20 ± 2 °C) and light-controlled environment (12 h light:12 h darkness cycle; lights on from 0600 h) with free access to food (Altromin 1324; Altromin, Lage, Germany) and water. After 1–2 weeks of acclimatization, the rats were subjected to the protocol approved by the Danish animal ethics committee to fulfil accepted standards of animal care.

Pre-surgery preparations

Catheters (Tygon Microbore S-50-HL tubing; Cole Parmer, Buch and Holm, Denmark) were sterilized with ethanol (70%) before surgery, and all surgical instruments were sterilized by heating (FST 250 Sterilizer; Fine Science Tools GmbH, Heidelberg, Germany) before use and during surgery. Prior to the operation, the jugular vein catheter (130 mm) and the left carotid artery catheter (160 mm) were filled with a solution of heparin (100 IU/ml; LEO, Copenhagen, Denmark) in saline and then a drop of silicone glue (primed with Grund G789 and followed by Elastosil E41; Wacker Chemie, Munchen, Germany) and a small, thin piece of cloth (polyester) were placed externally at a distance of 40 or 60 mm from the tip of the catheter respectively. The piece of cloth glued to the catheters ensured a tight fixation of the catheters to the vessels through adhesion to the connective tissue. Then rats were anesthetized with isoflurane (Abbott Scandinavia AB, Solna, Sweden) and given an analgesic treatment by s.c. injection of Anorfin (0·05 mg/kg; GEA, Frederiksberg, Denmark) and Rimadyl Vet (5 mg/kg; Pfizer, Ballerup, Denmark) followed by lidocain (Xylocain, 10 mg/incision; Astra, Göteborg, Sweden). Also, the animals were treated with antibiotics by i.m. injection of Streptocillin Vet (125 mg/kg dihydrostreptomycin and 100 000 IE/kg benzylpenicillinprocain; Boehringer Ingelheim, Dortmund, Germany).

Surgery

Abdominal artery via left carotid artery A 15 mm skin incision was made above the left carotid artery with a scalpel. The vessel was localized and uncovered with a pair of tweezers. A cut was made away from the heart with a small pair of scissors, while stasis of the blood was set in the other direction, and the catheter was inserted 50 mm into the abdominal artery.

Right jugular vein The vessel was exposed and prepared as above and the catheter was inserted 20–30 mm into the vessel. Both catheters were tunneled subcutaneously and exteriorized at the back of the neck using a needle (18G; Becton Dickinson, Dublin, Ireland), and the wounds were closed with suture (4/0; Johnson and Johnson, Woluwe, Belgium) and clips (Becton Dickinson).

Post-surgery operations

After surgery, the catheters were filled with a solution of heparin (500 IU; LEO) in Haemaccel (Hoechst, Frankfurt, Germany) and closed with 4 mm fishing line (diameter 0·45 mm). Then, the catheters were placed in a swivel device (DC105B, Instech Laboratories, Inc., Plymouth Meeting, PA, USA), filled with Streptocillin Vet (Boehringer Ingelheim), and the animals were returned to the animal facility and single housed. The rats were given an antibiotic and analgesic treatment for further 3 days. Then, 1 day prior to experiment, the arterial catheter was flushed with heparinized saline (100 IU/ml), and both catheters were filled with a solution of sodium citrate (6·8%) in Haemaccel. The infusion protocol was started only if full recovery was obtained, judged by the return of bodyweight to the pre-operational level.

Infusion protocol

Studies were performed on conscious unrestrained rats that were fasted overnight in their experimental cages. Then, on the morning of the experiment the animals were administered a single dose of glucose (2 mg/kg) or vehicle (saline, 4 ml/kg)

by oral gavage at $t=0$ min. At $t=30$ min, the infusion of tracer via the jugular vein was started and continued for 4 min. Small blood samples (160 μl) were drawn from the artery at $t=31$, 32, 33, 34, 35, 36, 38, 42, and 46 min for the determination of tracer concentrations (Oakes *et al.* 1999). Large blood samples (320 μl) were collected at $t=-2$, 27, and 46 min for the determination of plasma metabolites. All blood samples were collected in tubes coated with EDTA (2 mg/ml whole blood) and sodium fluoride (final plasma concentration of 1%). The measurements performed on the $t=-2$ min sample were considered a baseline value, while the average of the measurements from the 27 and 46 min samples was considered representative of the part of the post-administration period where tracer methodology was applied. After the collection of the final blood sample at $t=46$ min, the rats were killed by injection of 1 ml pentobarbital (0·1%). Tissues were then rapidly excised in the following order: heart, epididymal fat (white adipose tissue, WAT), liver, and white and red quadriceps muscle. Tissues were immediately freeze-clamped between a pair of aluminium tongs pre-cooled in liquid nitrogen and kept at −80 °C until subsequent analysis.

Synthesis of ^{3}H-R-BrP tracer

The (*R*)-2-bromopalmitate was synthesized as described in Oakes *et al.* (1999) with the following minor modification: the pure *R*-enantiomer was obtained by chromatographic resolution using 0·1% acetic acid in hexane as the mobile phase. By this method, 2·5 mCi product was obtained with radiochemical and chiral purity >98%, yield 15%.

Biochemical measurements

Plasma glucose, glycerol, and FFA were measured on a Hitachi 912 automatic analyzer (Boehringer Mannheim, Mannheim, Germany). Insulin was measured using a sandwich ELISA as previously described (Andersen *et al.* 1993).

ACC phosphorylation (ACC-p) in tissue homogenates was determined using the western blot technique. Briefly, tissue was homogenized and briefly centrifuged. The pellet was discarded and the supernatant stored in aliquots at −80 °C for subsequent determination of protein concentration and western blotting. Protein concentrations were determined using Bio-Rad protein assay (Bio-Rad) and using human serum albumin as standard. The primary antibody was an anti-phospho-ACC (Upstate, Charlottesville, VA, USA) and the secondary antibody was a horseradish peroxidase-labeled rabbit anti-goat antibody (Pierce Chemical, Rockford, IL, USA). The signal was detected using The LAS-3000 imaging system (Fuji Photo Film, Tokyo, Japan) and quantified using the Image Quant software (GE Healthcare, Uppsala, Sweden).

Determination of plasma and tissue tracer concentration

Tracer plasma and tissue content were determined as previously described (Oakes *et al.* 1999, Iglesias *et al.* 2004).

Calculation of rates of tissue FFA clearance, uptake and storage

Tissue clearance and uptake rates for ^{3}H-*R*-BrP and ^{14}C-P were calculated from the tissue content and plasma disappearance curves of these tracers, as previously described (Oakes *et al.* 1999, Furler *et al.* 2000, Hegarty *et al.* 2002). Incorporation of the metabolizable ^{14}C-P into the organic phase was used to calculate the clearance of FFA to lipid storage products (Kfs). Tissue entrapment of all ^{3}H radiolabel derived from the non-metabolizable ^{3}H-*R*-BrP was used to calculate the clearance Kf*, an index of total FFA clearance (Hegarty *et al.* 2002). Kf* and Rf* (the corresponding index of FFA uptake) are proportional to the actual clearance and uptake rates of circulating FFA (Oakes *et al.* 1999). However, because of different affinities of analog and authentic substrates for key metabolic processes, the constant of proportionality termed the lumped constant (LC*) is not unity. Appropriate values of LC* for different tissues of the conscious rat have previously been determined (Furler *et al.* 2000) and employed (Hegarty *et al.* 2002). Thus, to quantitatively compare total and storage components of fatty acid clearance the indices of total fatty acid clearance and uptake used here were Kf*/LC* and Rf*/LC* respectively.

The scaled clearance ratio (Kfs/(Kf*/LC*)) was also used. This ratio, the storage:uptake ratio, which provides an estimate of the proportion of FFA taken up by a tissue that is initially directed to storage, also included a LC* correction. Notably, the values of LC* used are not theoretical values but were determined from *in vivo* experiments, and are therefore subject to experimental error (Furler *et al.* 2000). The magnitude of the corrected parameters presented here should therefore be used as a guide only. Relative changes in parameters across experimental conditions will not be affected by any error in LC*. Also, it should be noted that our methodology quantifies only the initial disposition of plasma-derived FFA, which may not reflect its ultimate fate. Moreover, the technique does not yield a measure of the oxidation of fatty acid derived from intracellular stores, which would be required to determine absolute net rates of oxidation and storage. In the presentation of data, we have emphasized the clearance rates, since these are direct indicators of changes occurring in the tissues, whereas uptake rates are also a function of substrate availability.

Statistical analysis

Data are expressed as means±S.E.M. and compared by an unpaired Student's *t*-test, unless otherwise stated. $P<0·05$ was considered significant. All statistical calculations were

Table 1 Effect of glucose on plasma parameters

	Vehicle		Glucose	
	Baseline	Post-administration	Baseline	Post-administration
FFA (μM)	456±38	397±21	451±38	148±20*
Glycerol (μM)	0·13±0·01	0·11±0·01	0·13±0·01	0·07±0·01†
Glucose (mM)	5·2±0·2	5·7±0·2	5·2±0·1	9·1±0·4*
Insulin (pM)	48±24	54±12	49±11	233±36*

Plasma levels of FFA, glycerol, glucose, and insulin at baseline and post-administration of vehicle control (saline) or glucose to overnight-fasted rats are shown. Data are given as means±S.E.M. with $n=5$ per group. Statistics: in each treatment group, the baseline values were compared with post-administration values by a paired Student's *t*-test; *$P<0·001$, †$P<0·01$.

performed using GraphPad Prism version 3.03 (GraphPad Software, Inc., San Diego, CA, USA).

Results

Bodyweight (vehicle, 289±4 g; glucose, 291±7 g) and baseline plasma levels of glucose, insulin, FFA, and glycerol did not differ significantly across treatment groups ($P=$not significant (n.s.), Table 1). Plasma levels of glucose, insulin, FFA, and glycerol did not change significantly with administration of vehicle. In contrast, oral administration of glucose caused an almost twofold increase in the plasma glucose level ($P<0·001$), which was accompanied by an almost fivefold increase in plasma insulin levels ($P<0·001$). Also, glucose administration caused a suppression of plasma levels of FFA by 70% ($P<0·001$), which was accompanied by a decrease in plasma levels of glycerol of approximately 40% ($P<0·01$).

Acute oral administration of glucose did not affect the total FFA clearance rate in liver, red and white muscles, or in WAT (Fig. 1) as compared with vehicle control. In contrast, in heart (Table 2), the total FFA clearance rate was clearly increased in rats administrated with glucose compared with vehicle control ($P<0·01$). Clearance rates of FFA into storage (Fig. 2) were decreased in WAT ($P<0·05$) and increased in liver ($P<0·05$), whereas in all other tissues the clearance rates of FFA into storage were equal ($P=$n.s.), when comparing glucose-treated rats with vehicle control. The corresponding rates of FFA uptake and storage are summarized in Table 3.

We calculated the storage:uptake ratio as an index of the intracellular partitioning of FFA (Fig. 3, Table 2). Administration of glucose directed the partitioning of FFA toward

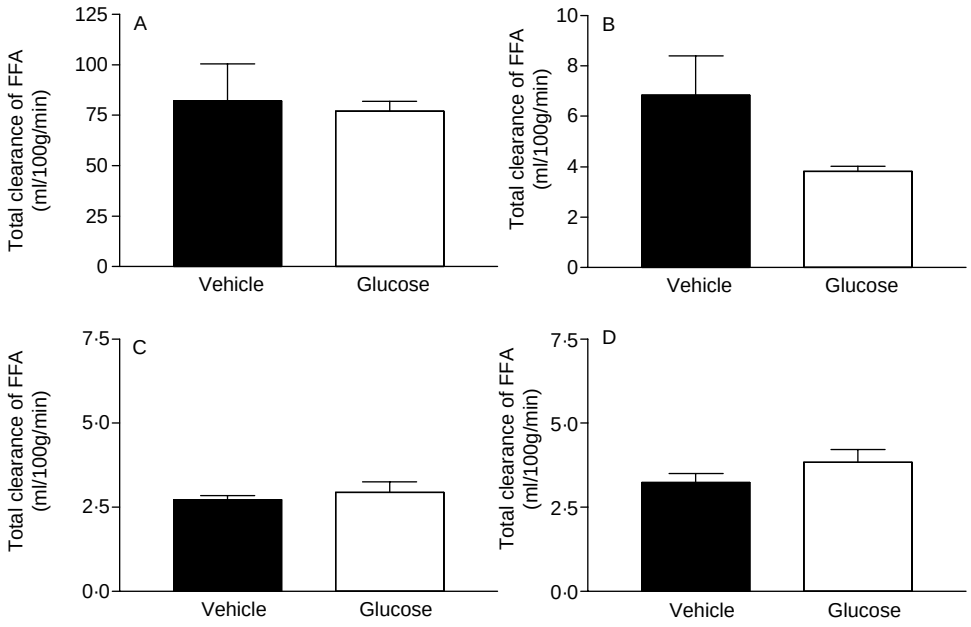

Figure 1 The effect of glucose on total tissue clearance of FFA. The effects of vehicle control (solid bars) or glucose (open bars) on the total FFA clearance in (A) liver, (B) white adipose tissue, (C) white muscle, and (D) red muscle in overnight-fasted rats were determined. Initial tissue FFA clearance was determined by measuring ^{3}H-*R*-BrP content against the area of the plasma disappearance curve of this tracer, see Materials and Methods for details. Data are shown as means±S.E.M. with $n=5$ per group.

Table 2 Effect of glucose on FFA utilization in heart

	Vehicle	Glucose
Total FFA clearance (ml/100 g/min)	25·8±5·0	62·6±5·4*
Clearance of FFA into storage (ml/100 g/min)	8·5±1·0	13·4±2·1
Storage:uptake ratio	0·36±0·04	0·22±0·02†

The effects of vehicle control or glucose on total FFA clearance and clearance of FFA into storage rates in heart. Also given are the storage:uptake ratios. Total tissue FFA clearance was determined by ^{3}H-*R*-BrP content against the area of the plasma disappearance curve of this tracer, while tissue clearance of FFA into storage was determined by measuring ^{14}C-palmitate content in the extracted lipid pool against the area of the plasma disappearance curve of this tracer, see Materials and Methods for details. Data are given as means±S.E.M. with $n=5$ per group; *$P<0·01$; †$P<0·05$.

storage in white quadriceps muscle (vehicle vs glucose; 0·64±0·02 vs 0·92±0·09, $P<0·05$) and in liver (0·66±0·07 vs 0·98±0·04, $P<0·01$), but not in red quadriceps muscle (1·18±0·07 vs 1·36±0·11, P=n.s.), or in WAT (P=n.s.). In contrast, in heart, administration of glucose directed the partitioning of FFA toward oxidation (0·36±0·04 vs 0·22±0·09, $P<0·001$).

We measured the phosphorylation state of ACC in liver and white and red quadriceps muscle (Table 4). We observed no differences in glucose-administered rats as compared with vehicle control (P=n.s.).

Discussion

In this study, we have investigated an aspect of the so-called 'reverse' Randle effect, where elevated glucose flux and oxidation in tissues are thought to impinge on fatty acid metabolism essentially leading to a relatively decreased degree of intracellular fatty acid oxidation. Previously, Sidossis *et al.* have pointed towards a direct role of glucose on whole-body fatty acid oxidation, by demonstrating that availability of glucose and insulin-shunted FA-CoA away from oxidation and towards storage in human muscle. The mechanism was proposed to involve inhibition of CPT-I activity by increased levels of malonyl-CoA generated from oxidation of glucose (Sidossis *et al.* 1996, Rasmussen *et al.* 2002).

We have now extended these findings using a novel tracer technique (Oakes *et al.* 1999, Hegarty *et al.* 2002, Oakes & Furler 2002) that allows assessment of the 'reverse' Randle cycle in individual tissues, including distinct muscle types in the rat. There was some prior evidence to suggest that the 'reverse' Randle cycle may function differently in red and white muscles, but this phenomenon had not been directly investigated. For example, pharmacological activation of AMPK, an indirect stimulator of the mitochondrial fatty acid transport process, leads to a more pronounced response in white than red muscle (Buhl *et al.* 2001, Iglesias *et al.* 2002, 2004). We now show that when plasma glucose and insulin are physiologically elevated, there was a clear increase in

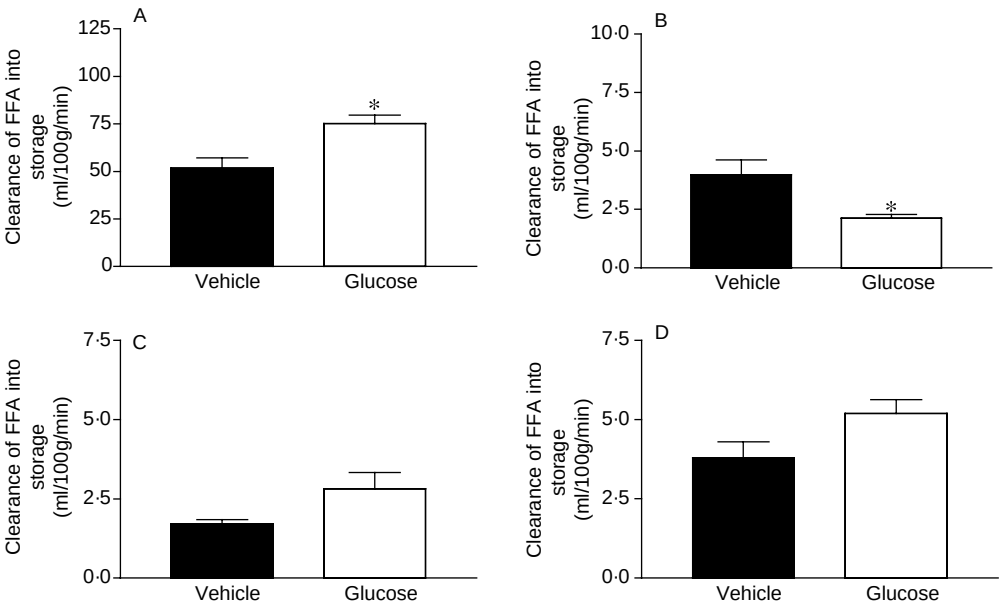

Figure 2 The effect of glucose on tissue clearance of FFA into storage. The effects of vehicle control (solid bars) or glucose (open bars) on the clearance of FFA into storage in (A) liver, (B) white adipose tissue, (C) white muscle, and (D) red muscle in overnight-fasted rats were determined. Initial tissue clearance of FFA into storage was determined by measuring ^{14}C-P content in the extracted lipid pool against the area of the plasma disappearance curve of this tracer, see Materials and Methods for details. Data are shown as means±S.E.M. with $n=5$ per group; *$P<0·05$.

Table 3 Effect of glucose on tissue uptake and storage rates of FFA

	Uptake rate (μmol/100 g/min)		Storage rate (μmol/100 g/min)	
	Vehicle	Glucose	Vehicle	Glucose
Liver	32·5±7·5	11·5±1·9*	20·4±2·8	11·3±1·9*
WAT	2·7±0·6	0·6±0·1*	1·6±0·3	0·3±0·03†
White muscle	1·1±0·1	0·4±0·04‡	0·7±0·1	0·4±0·1†
Red muscle	1·3±0·2	0·6±0·1*	1·6±0·3	0·8±0·1*
Heart	10·0±1·6	8·9±0·7	3·4±0·4	1·8±0·1*

The effects of vehicle control or glucose on FFA uptake and storage rates in liver, white adipose tissue (WAT), white and red quadriceps muscle, and heart are shown. Storage and uptake rates were calculated based on the rates of total clearance of FFA, clearance of FFA into storage, and plasma levels of FFA, see Materials and Methods for details. Data are given as means±S.E.M. with $n=5$ per group; *$P<0·05$; †$P<0·01$; ‡$P<0·001$.

partitioning of FFA towards storage in white but not red muscle.

Our data suggest that white muscle may be more sensitive towards acute changes in glucose and insulin availability, this despite a reported quantitatively greater insulin-mediated glucose uptake in red muscle compared with white muscle (Buhl *et al.* 2001, Iglesias *et al.* 2002). The mechanism responsible for this observation is not clear at present and should be further addressed. It is possible that there are differences between red and white muscles with respect to regulation of fatty acid oxidation via the AMPK–malonyl-CoA network in response to elevated glucose flux. Glucose and/or insulin are known to modulate individual components of this system. Glucose increases the concentration of citrate, an allosteric activator of ACC (Saha *et al.* 1997) and decreases the activity of AMPK (Itani *et al.* 2003). Here, we measured the ACC-p state as a measure of the AMPK activity/CPT-I axis (Park *et al.* 2002). We were not able to detect any effect of the glucose administration in white or red muscle, or in liver, possibly because the enzyme returned to the more dephosphorylated state before the collection of tissues, and therefore it remains unknown whether the differences between muscle types can be explained by the AMPK–malonyl-CoA network. However, the differences between muscle types in our results could also be due to the numerous other factors known to influence FFA partitioning. For example, insulin is thought to promote FFA storage directly in non-adipose as well as adipose tissues (Vila *et al.* 1990) while different isoforms of acyl-CoA synthase and/or fatty acid transporters may promote either FFA oxidation or storage (Bonen *et al.* 2000, Kim *et al.* 2004, Fisher & Gertow 2005).

The present results in muscle differ from our previous study using the euglycemic/hyperinsulinemic clamp technique (Hegarty *et al.* 2002). In that study, where plasma insulin, but not glucose was elevated, FFA was partitioned towards storage in liver but not in skeletal muscle. This suggests that there may be disparate effects of elevated glucose and insulin on FFA partitioning. However, a definitive answer would require a series of experiments specifically designed to answer this question. Such experiments would require that glucose

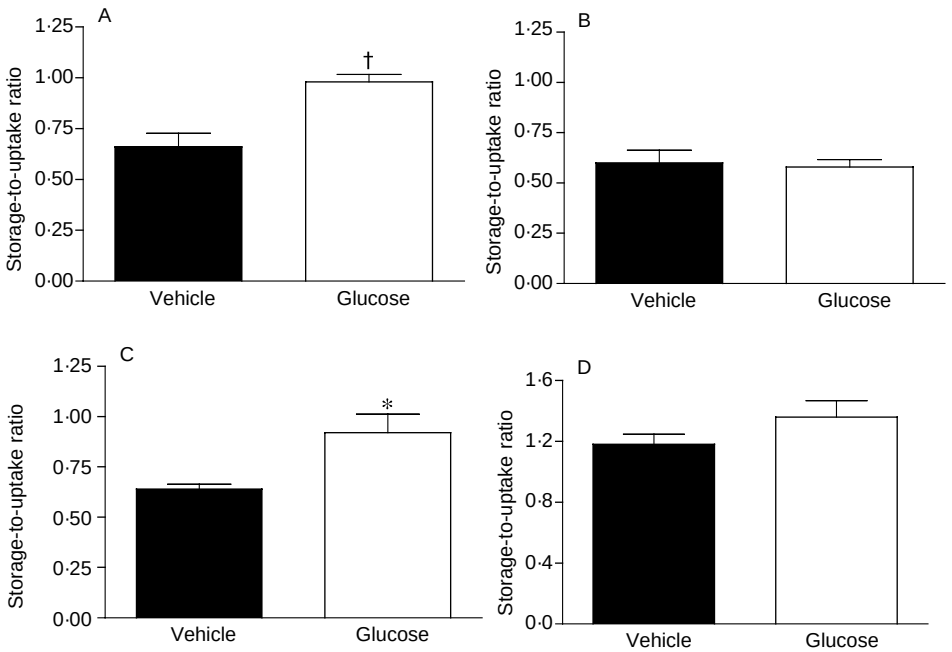

Figure 3 The effect of glucose on tissue fatty acid storage:uptake ratio. The effects of vehicle control (solid bars) or glucose (open bars) on the FFA storage:uptake ratio in (A) liver, (B) white adipose tissue, (C) white muscle, and (D) red muscle in overnight-fasted rats were determined. Data are shown as means±S.E.M. with $n=5$ per group; *$P<0·05$; †$P<0·01$ vs vehicle.

Table 4 Effect of glucose on acetyl-CoA carboxylase phosphorylation state

	ACC-p (% of standard)	
	Vehicle	Glucose
Liver	94±6	93±3
White muscle	287±45	255±29
Red muscle	436±45	375±35

The effects of vehicle control or glucose on ACC phosphorylation state in liver, white and red quadriceps muscle are shown, see Materials and Methods for details. Data are given as means±S.E.M. with $n=5$ per group.

flux into a tissue of interest was maintained constant, while plasma glucose and insulin levels were manipulated independently. These complex mechanistic studies are beyond the scope of the present investigation. Here, we only sought to investigate the effects of a physiological elevation of glucose and insulin on FFA partitioning.

It has been known for several years that insulin in the isolated perfused liver promotes an increase in fatty acid esterification and a decrease in fatty acid oxidation (Topping & Mayes 1972). Here, we confirm *in vivo* that glucose promotes intracellular partitioning towards storage in the liver. In contrast, we observed no effect of glucose administration on the intracellular partitioning of FFA in WAT, while both total clearance of FFA and clearance of FFA into storage were decreased. The reason for the difference between the responses of the different organs is not clear at present.

We also included heart in the study, since this tissue is a significant FFA consuming organ under normal conditions (Oakes *et al.* 1999). Interestingly, in heart, administration of glucose caused a dramatic increase in the total clearance of FFA, and the initial intracellular partitioning of FFA towards storage was decreased in the glucose-treated group compared with vehicle (Table 2). The data indicate a preferential use of FFA as a substrate for oxidation in heart and a unique regulation of the partitioning of fatty acid compared with the other tissues also studied here. The mechanism underlying this heart phenomenon is not known at present, but should be further addressed. Methodologically, it is possible that, in contrast to other tissues, cardiac ^{3}H-*R*-BrP uptake may reflect FFA oxidation rather than total FFA uptake (Oakes *et al.* 2006). However, if this were the case it does not invalidate the use of the clearance ratio presented here as a quantitative index of initial intracellular partitioning of FFA.

It may be argued that the effect on FFA partitioning following glucose administration is caused by the observed decrease in plasma FFA levels (Table 1). However, we have previously reported that local factors not determined by systemic availability can modulate FFA partitioning (Furler *et al.* 2000). Moreover, in additional studies not reported here, we have shown that decreasing plasma FFA levels with the lipolysis inhibitor acipimox, rather than by elevating insulin, has no effect on FFA partitioning (K Fosgerau, unpublished observations).

In summary, we have shown that the effect of physiological elevation of glucose and insulin does in fact alter the initial intracellular partitioning of FFA *in vivo*, but that the degree of partitioning is tissue specific. Fatty acid is preferentially channeled towards storage in liver and white, but not red, muscle and adipose tissue. Moreover in heart, elevated glucose flux decreases the proportion of FFA directed to storage. These results suggest that lipid accumulation in non-adipose tissues (and resulting pathologies) could be promoted by only mild abnormalities in glucose metabolism. Conversely, it is likely that the excess lipid accumulation could be prevented by therapies aimed at modulating the interaction of glucose and lipid metabolism. However, our results imply that such therapies would be most effective in white muscle and liver.

Acknowledgements

The expert technical assistance of Helle Petersen, Aase Vinterby, Lone Sørensen, Pia Justensen, and Jesper Damgaard is gratefully acknowledged. Also these authors wish to thank Drs Ji-Ming Ye and Gregory J Cooney for comments and fruitful discussions of the present work. The authors declare that there is no conflict of interest that would prejudice the impartiality of this scientific work.

References

Andersen L, Dinesen B, Jørgensen PN, Poulsen F & Røder M E 1993 Enzyme immunoassay for intact human insulin in serum or plasma. *Clinical Chemistry* **39** 578–582.

Bonen A, Luiken JJ, Arumugam Y, Glatz JF & Tandon NN 2000 Acute regulation of fatty acid uptake involves the cellular redistribution of fatty acid translocase. *Journal of Biological Chemistry* **275** 14501–14508.

Buhl ES, Jessen N, Schmitz O, Pedersen SB, Pedersen O, Holman GD & Lund S 2001 Chronic treatment with 5-aminoimidazole-4-carboxamide-1-beta-D-ribofuranoside increases insulin-stimulated glucose uptake and GLUT4 translocation in rat skeletal muscles in a fiber type-specific manner. *Diabetes* **50** 12–17.

Fisher RM & Gertow K 2005 Fatty acid transport proteins and insulin resistance. *Current Opinion in Lipidology* **16** 173–178.

Furler SM, Cooney GJ, Hegarty BD, Lim-Fraser MY, Kraegen EW & Oakes ND 2000 Local factors modulate tissue-specific NEFA utilization: assessment in rats using ^{3}H-(*R*)-2-bromopalmitate. *Diabetes* **49** 1427–1433.

Hardie DG & Carling D 1997 The AMP-activated protein kinase–fuel gauge of the mammalian cell? *European Journal of Biochemistry* **246** 259–273.

Hegarty BD, Cooney GJ, Kraegen EW & Furler SM 2002 Increased efficiency of fatty acid uptake contributes to lipid accumulation in skeletal muscle of high fat-fed insulin-resistant rats. *Diabetes* **51** 1477–1484.

Hegarty BD, Furler SM, Ye J, Cooney GJ & Kraegen EW 2003 The role of intramuscular lipid in insulin resistance. *Acta Physiologica Scandinavica* **178** 373–383.

Iglesias MA, Ye JM, Frangioudakis G, Saha AK, Tomas E, Ruderman NB, Cooney GJ & Kraegen EW 2002 AICAR administration causes an apparent enhancement of muscle and liver insulin action in insulin-resistant high-fat-fed rats. *Diabetes* **51** 2886–2894.

Iglesias MA, Furler SM, Cooney GJ, Kraegen EW & Ye JM 2004 AMP-activated protein kinase activation by AICAR increases both muscle fatty acid and glucose uptake in white muscle of insulin-resistant rats *in vivo*. *Diabetes* **53** 1649–1654.

Itani SI, Saha AK, Kurowski TG, Coffin HR, Tornheim K & Ruderman NB 2003 Glucose autoregulates its uptake in skeletal muscle: involvement of AMP-activated protein kinase. *Diabetes* **52** 1635–1640.

Kelley DE & Goodpaster BH 2001 Skeletal muscle triglyceride. An aspect of regional adiposity and insulin resistance. *Diabetes Care* **24** 933–941.

Kim JK, Gimeno RE, Higashimori T, Kim HJ, Choi H, Punreddy S, Mozell RL, Tan G, Stricker-Krongrad A, Hirsch DJ *et al*. 2004 Inactivation of fatty acid transport protein 1 prevents fat-induced insulin resistance in skeletal muscle. *Journal of Clinical Investigation* **113** 756–763.

Oakes ND & Furler SM 2002 Evaluation of free fatty acid metabolism *in vivo*. *Annals of the New York Academy of Sciences* **967** 158–175.

Oakes ND, Kjellstedt A, Forsberg GB, Clementz T, Camejo G, Furler SM, Kraegen EW, Olwegard-Halvarsson M, Jenkins AB & Ljung B 1999 Development and initial evaluation of a novel method for assessing tissue-specific plasma free fatty acid utilization *in vivo* using (R)-2-bromopalmitate tracer. *Journal of Lipid Research* **40** 1155–1169.

Oakes ND, Thalen P, Aasum E, Edgley AJ, Larsen TS, Furler SM, Ljung B & Severson DL 2006 Cardiac metabolism in mice: tracer method developments and *in vivo* application revealing profound metabolic inflexibility in diabetes. *American Journal of Physiology – Endocrinology and Metabolism* **290** E870–E881.

Park SH, Gammon SR, Knippers JD, Paulsen SR, Rubink DS & Winder WW 2002 Phosphorylation-activity relationships of AMPK and acetyl-CoA in muscle. *Journal of Applied Physiology* **92** 2475–2482.

Rasmussen BB, Holmback UC, Volpi E, Morio-Liondore B, Paddon-Jones D & Wolfe RR 2002 Malonyl coenzyme A and the regulation of functional carnitine palmitoyltransferase-1 activity and fat oxidation in human skeletal muscle. *Journal of Clinical Investigation* **110** 1687–1693.

Saha AK, Vavvas D, Kurowski TG, Apazidis A, Witters LA, Shafrir E & Ruderman NB 1997 Malonyl-CoA regulation in skeletal muscle: its link to cell citrate and the glucose-fatty acid cycle. *American Journal of Physiology* **272** E641–E648.

Sidossis LS, Stuart CA, Shulman GI, Lopaschuk GD & Wolfe RR 1996 Glucose plus insulin regulate fat oxidation by controlling the rate of fatty acid entry into the mitochondria. *Journal of Clinical Investigation* **98** 2244–2250.

Topping DL & Mayes PA 1972 The immediate effects of insulin and fructose on the metabolism of the perfused liver. Changes in lipoprotein secretion, fatty acid oxidation and esterification, lipogenesis and carbohydrate metabolism. *Biochemical Journal* **126** 295–311.

Vila MC, Milligan G, Standaert ML & Farese RV 1990 Insulin activates glycerol-3-phosphate acyltransferase (*de novo* phosphatidic acid synthesis) through a phospholipid-derived mediator. Apparent involvement of Gi alpha and activation of a phospholipase C. *Biochemistry* **29** 8735–8740.

Received 14 February 2006
Received in final form 4 May 2006
Accepted 26 May 2006
Made available online as an Accepted Preprint
23 June 2006